# Pulsatile Cerebrospinal Fluid Dynamics in the Human Brain

Andreas A. Linninger*, Cristian Tsakiris, David C. Zhu, Michalis Xenos, Peter Roycewicz, Zachary Danziger, and Richard Penn

***Abstract*—Disturbances of the cerebrospinal fluid (CSF) flow in the brain can lead to hydrocephalus, a condition affecting thousands of people annually in the US. Considerable controversy exists about fluid and pressure dynamics, and about how the brain responds to changes in flow patterns and compression in hydrocephalus. This paper presents a new model based on the first principles of fluid mechanics. This model of fluid-structure interactions predicts flows and pressures throughout the brain's ventricular pathways consistent with both animal intracranial pressure (ICP) measurements and human CINE phase-contrast magnetic resonance imaging data. The computations provide approximations of the tissue deformations of the brain parenchyma. The model also quantifies the pulsatile CSF motion including flow reversal in the aqueduct as well as the changes in ICPs due to brain tissue compression. It does not require the existence of large transmural pressure differences as the force for ventricular expansion. Finally, the new model gives an explanation of communicating hydrocephalus and the phenomenon of asymmetric hydrocephalus.**

***Index Terms*—CSF flow, fluid-structure interactions, hydrocephalus, intracranial pressure, tissue compliance.**

## NOMENCLATURE

| | |
|---|---|
| $A_i$ | Cross section of the ventricular or subarachnoid section [$m^2$]. |
| $a(t)$ | Choroid plexus displacement [m]. |
| $h_i$ | Height of the ventricular or subarachnoid section [m]. |
| $k_e$ | Tissue elasticity constant [N/m]. |
| $k_d$ | Tissue compliance [(N s)/m]. |
| $F_i$ | Poiseuille Friction term [N/$m^3$]. |
| $l_i$ | Length of foramina connecting ventricles [m]. |
| $p_0(t)$ | Pressure of brain parenchyma [N/$m^2$]. |
| $p_i(t), p_{\mathrm{SAS}}(t)$ | CSF pressure in ventricles and subarachnoid section—ICP [N/$m^2$]. |
| $q_{e,j}(t)$ | Reabsorption flow rate in a section [$m^3$/s]. |
| $q_{f,i}(t)$ | CSF production rate in the choroid plexus [$m^3$/s]. |
| $q_i(t) = A_i v_i$ | CSF flow rate leaving ventricle, i.e., flow in formina and aqueduct [$m^3$/s]. |
| $r_i$ | Radius of the foramina and aqueduct [m]. |
| $v_i(t)$ | Axial CSF flow velocity [m/s]. |
| $y_i(t)$ | Tissue displacement in a section [m]. |

Greek Symbols

| | |
|---|---|
| $\alpha$ | Amplitude of choroid expansion [m]. |
| $\delta$ | Tissue width [m]. |
| $\kappa$ | Reabsorption constant [$m^3$/(Pa s)]. |
| $\mu$ | Fluid Viscosity [Pa s]. |
| $\rho$ | Fluid density [kg/$m^3$]. |
| $\rho_w$ | Tissue density [kg/$m^3$]. |
| $\omega$ | Heart rate frequency [rad/s]. |

Manuscript received March 12, 2004; revised August 29, 2004. *Asterisk indicates corresponding author.*

*A. A. Linninger is with the Laboratory for Product and Process Design (LPPD), Department of Chemical Engineering, University of Illinois at Chicago 810 S. Clinton Street, CEB 216, Chicago, IL 60607 USA (e-mail: linninge@uic.edu).

C. Tsakiris, M. Xenos, P. Roycewicz, and Z. Danziger are with the Laboratory for Product and Process Design (LPPD), Department of Chemical Engineering, University of Illinois at Chicago, Chicago, IL 60607 USA.

D. C. Zhu is with the Department of Radiology, University of Chicago, Chicago, IL 60607 USA.

R. Penn is with the Department of Neurosurgery, University of Chicago, Chicago, IL 60607 USA.

Digital Object Identifier 10.1109/TBME.2005.844021

## I. INTRODUCTION

IN 1976, Hakim [1] proposed an important model of the brain as a sponge, postulating that large transmural pressure differences between the SAS and ventricles cause ventricular enlargement by squeezing water out of the brain parenchyma. While this may occur in obstructive hydrocephalus in which a tumor or injury blocks the proximal CSF pathways, large pressure gradients predicted by Hakim are not consistent with the open foramina in communicating hydrocephalus. Furthermore, Hakim's hypothesis cannot explain why the intracranial pressure (ICP) often returns to almost normal levels in patients with communicating hydrocephalus.

An understanding of the basic underlying fluid mechanics in the normal brain and in hydrocephalus is needed to develop more effective medical treatments. In particular, the pulsatile flow rates, ICPs, pressure gradients, and their interaction with each other need to be understood in order to design CSF shunting systems which compensate correctly for the fluid dynamic abnormalities.

This paper presents a comprehensive computational model of normal and hydrocephalic CSF flow. The first section reviews experiments on dogs that show CSF flow is pulsatile and large pressure gradients are not present. The second section proposes a mathematical model of intracranial dynamics based on first principles of fluid mechanics. The third section presents simulation results for normal CSF flow and demonstrates conditions leading to hydrocephalus. The validation section provides experimental evidence to support the proposed mechanisms, and validates the simplified assumptions of using two-dimensional

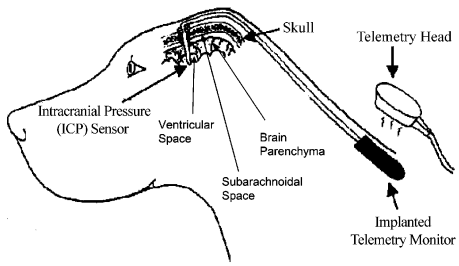


Fig. 1. Placement of ICP monitors in dog experiments. (Only one monitor is shown for clarity.).

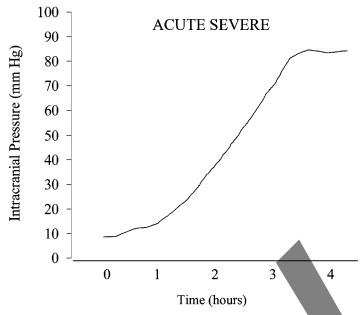


Fig. 2. Experimental ICP increments measured in an acutely hydrocephalic dog. (Pulse pressure not shown in this chronic record.).

(2-D) computational fluid dynamic (CFD) simulations. The simulations are also compared with data from CINE phase-contrast magnetic resonance imaging (MRI).

## II. Animal Experiments

A series of experiments on dogs was performed to establish the role of ICP gradients in communicating hydrocephalus. Multiple INSITE pressure sensors (Medtronic, Inc., Minneapolis, MN) were implanted for simultaneous *in vivo* measurements. This new technique generated both long-term and real-time ICP measurements. The sensors were placed in three different locations: the lateral ventricle, the brain parenchyma, and the SAS as shown in Fig. 1. Real-time measurements were obtained at 256 ICP data points per second. Long-term ICP trends were recorded for a period of 20 days with the average pressure sampled every 5 min. A more detailed description of the experiments is given elsewhere [2].

Six dogs were injected cisternally with kaolin to induce hydrocephalus. In one dog, the ICP rose rapidly both in the absolute value and in the pulse pressure, peaking at about 10 000 Pa (∼70 Torr) above normal (Fig. 2). The huge ICP rise was fatal to this dog within 16 h. The autopsy of the animal showed expanded ventricles consistent with acute communicating hydrocephalus. The SAS was found to be clogged with kaolin. In effect, kaolin injection blocked the CSF reabsorption through the SAS. This dog's ventricular expansion appears to be a consequence of CSF accumulation. The duration for reaching the peak ICP is consistent with CSF accumulation at constant production, with minimal reabsorption [3], [4].

In four dogs, chronic hydrocephalus was induced. Both the long-term and real-time data from simultaneous recordings failed to show any measurable pressure gradients across the ventricle to the parenchyma or the SAS to the parenchyma (Fig. 3). Autopsy confirmed moderate hydrocephalus in all four dogs. One dog did not develop chronic hydrocephalus, and died with seizures after a second kaolin injection.

The experimental data show that the ICP is pulsatile with a peak in systole and a valley in diastole. The synchronization of CSF pressure with the cardiac cycle corroborates the clinical evidence linking CSF motion in the ventricular system to arterial pulsations. Recently, Egnor [5] has proposed that pulsatile choroid plexus motion due to arterial pulsations actively powers the CSF's oscillatory motion in the ventricles.

In Hakim's hypothesis, transmural pressure gradients across the parenchyma are essential for explaining ventricular expansion [1]. However, in our experiment such large pressure differences were not found. In fact, no transmural pressure differences in our dogs were seen, see Fig. 3. If pressure differences do exist, they are below 1–2 Torr (133–267 Pa), the sensitivity of the ICP monitors. Our first principles analysis in the next section will provide an explanation why large transmural pressure differences cannot develop with open ventricular pathways.

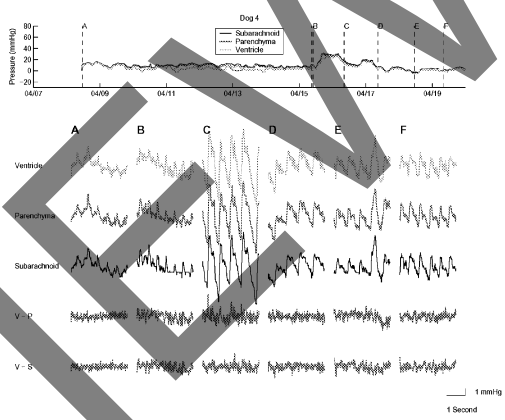


Fig. 3. Long-term ICP chronic hydrocephalic dog and real-time pressure difference between ventricles and parenchyma (V-P) and ventricles and SAS (V-S). The top graph shows chronic recordings prior to kaolin injection (up to B) and then after as the ICP elevates and returns to normal with the development of hydrocephalus. The middle three records are the real-time pressure of the ventricle, parenchyma and SAS. The lower two are subtractions of ventricle minus parenchmyma pressure (V-P) and ventricle minus SAS pressure (V-S). No significant pressure gradient is observed.

## III. Modeling of the CSF Dynamics

CSF oscillatory flow results from cardiac pulsations ([1], [5]–[7]). The pattern and timing of CSF motion has been studied extensively with MRI techniques ([6]–[9]). Nevertheless, the causes and mechanical principles underlying intracranial dynamics are controversial. Some authors link the CSF flow to the brain motion. This hypothesis is supported by careful measurements of brain motion using CINE phase-contrast MRI, [9]–[11]. Other investigators suggest a pulsatory thalamic pump actively pushing the CSF [12]. A competing view attributes CSF motion to a transmission of the arterial pressure in the choroid plexus. Another study, which combined gated MR with automated edge-detection algorithms, observed a 10%–20% variation in size of the lateral ventricles during the normal cardiac cycle [13]. These measurements are not consistent with the brain motion hypothesis according to which arterial pulsation should diminish the ventricular size in the systole.

The critical role of the choroid plexus in the development of communicating hydrocephalus was established by Bering [14]. In dogs injected with kaolin, he found that only ventricles with an intact choroid plexus expanded. If the choroid plexus had been removed, the ventricle did not enlarge. Thus, the choroid plexus is necessary for ventricular expansion in communicating hydrocephalus.

All these phenomena, including arterial expansion, brain motion and choroid expansion are likely to contribute to some extent. In order to understand intracranial dynamics better, a mathematical model quantifying forces and their interaction is needed to evaluate the different hypotheses. This section introduces a model based on the first principles of fluid mechanics which is designed to calculate stresses, strains and displacement in the cranial cavity. We made the choroid plexus as the principal driver of CSF motion. The effects of complex brain motion resulting from cardiac pulsations transmitted to the intracranial space [9] are not difficult to incorporate into our bio-mechanical model.

The first principles model for pulsatile CSF flow relates three dynamically interacting systems: the cerebral vascular system, the CSF-filled ventricular and SAS, and the brain parenchyma. Fig. 4 illustrates how the CSF pulsatile motion in the ventricular system occurs in our view. Arterial blood flows into the distensible tissues of the choroid plexus cause it to expand during systole. Simultaneously, new CSF is produced in the choroid plexus by secretion at a constant rate ([14]–[18]). Thus, the choroid plexus acts like a pump, and drives the pulsatile CSF circulation. The transient velocities and pressure field in turn lead to periodic compression of the brain parenchyma observable as ventricular pulsations.

Fig. 5 is a schematic of the CSF pathways interacting with the vascular system and the parenchyma. The CSF traverses the lateral ventricles (V1 and V2), the foramina of Monro (FM), the third ventricle (V3), and flows into the fourth ventricle (V4) through the aqueduct of Sylvius (AS), and then finally reaches the subarachnoid space (SAS) through the foramina of Luschke (FL) and Magendie (FMa). In the SAS, CSF is reabsorbed into the sagittal sinus along the top of the cranium and also in the spinal canal. The pulsatile CSF motion is effectively powered by the kinetic energy of the arterial pump of the choroid plexus. The expansion and compression of the parenchyma influences the blood perfusion and, thus, provides a feedback loop on the CSF dynamics [19].

The goal of our detailed hydrodynamic modeling is to compute the CSF pressure and velocity fields throughout the brain for comparison with clinical data. The fluid motion obeys the continuity and the Navier–Stokes equations. The dynamics of parenchyma stresses, strains and displacements can be described with the laws of elastodynamics. At the interface of the fluid and the elastic tissue, the boundary conditions dictate equality of displacements and stresses. Since the deformation of the tissues directly affects the space available to the fluid, the two systems are fully coupled. Instead of directly resolving the complex three-dimensional (3-D) dynamic brain deformation problem with fluid-structure interaction, a few assumptions are taken to simplify the mathematics. Theses assumptions will be justified in the validation section by means of a commercial CFD tool [20].

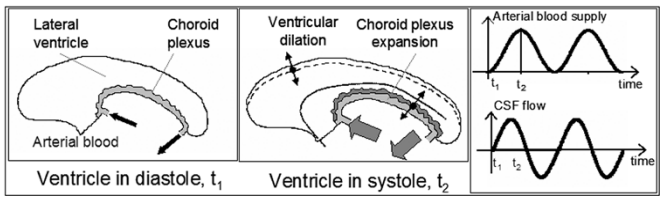


Fig. 4. CSF flow due to the choroid plexus.

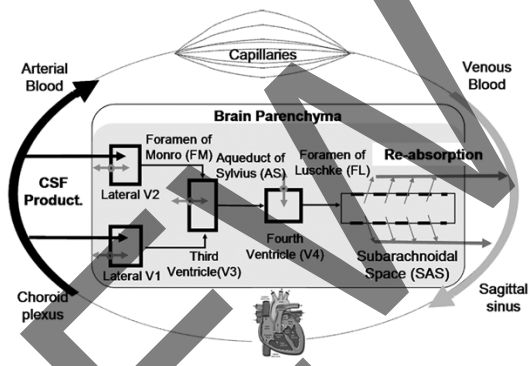


Fig. 5. Schematic of CSF pathways, the vascular system and brain parenchyma.

The initial mathematical framework for one-dimensional (1-D) intracranial dynamics is as follows. The forces and displacements for each ventricle interacting with the elastic brain tissues are depicted in Fig. 6. A difference in fluid $(p_i)$ and intracranial tissue pressure $(p_0)$ causes the extension of the ventricular wall. In this first approach, only a thin layer of epithelial cells in the peri-ventricular area is included. This simplification allows adopting the standard thin elastic membrane model of tissue deformation [21]. The acceleration of a small membrane segment results from the interaction of three forces: the difference between fluid and tissue pressures $(p_i - p_0)$, the tissue elasticity $(k_e \cdot y_i)$ as well as a dissipative force $(k_d \cdot \dot{y}_i)$. The interior of the ventricle is compressed by the choroid plexus. The cyclic motion of choroid plexus follows the cardiac cycle and is represented by the forcing function $a(t)$ given in (1)

$$a(t) = \alpha \left(1.3 + \sin\left(\omega t - \frac{\pi}{2}\right) - \frac{1}{2}\cos\left(2\omega t - \frac{\pi}{2}\right)\right). \quad (1)$$

In ensemble, the relative dynamics of choroid expansion $a(t)$ and the induced tissue expansion $y_i(t)$ determine the instantaneous CSF content in the ventricle as well as the CSF flow rate along the proximal pathways at each instant of time. To resolve the ventricular dynamics better, the ventricles were also discretized into cylindrical finite volumes with perfect axial dispersion and radial expandability against the thin periventricular membrane [22], see Fig. 6. The foramina are treated as elastic tubes. Since the diameters of all foramina are small, averaged axial velocities $(v_i)$ were considered in the momentum balances. The radial CSF momentum balance in the thin foramina was neglected. The radial velocity components equal to the tissue deformation speed $\dot{y}_i$ appear in the continuity